Supporting information

Charge transfer dynamics and catalytic performance of a covalently linked hybrid assembly comprising a functionalized cobalt tetraazamacrocyclic catalyst and $CuInS_2$/ZnS quantum dots for photochemical hydrogen production

Chengming Nie,[a] Wenjun Ni,[a] Lunlun Gong,[a] Jian Jiang,[a] Junhui Wang*[b] and Mei Wang*[a]

[a]*State Key Laboratory of Fine Chemicals, Institute of Artificial Photosynthesis, Dalian University of Technology, Dalian 116024, China. E-mail: symbueno@dlut.edu.cn (M.W.)*
[b]*State Key Laboratory of Molecular Reaction Dynamics and Collaborative Innovation Center of Chemistry for Energy Materials (iChEM), Dalian Institute of Chemical Physics, Chinese Academy of Sciences, Dalian 116023, China. E-mail: wjh@dicp.ac.cn (J.W)*

Experimental details

Materials

L-Glutathione reduced (98%), copper nitrate dihydrate (99.99%), indium chloride anhydrous (99.99%), zinc acetate dihydrate (99%), sodium sulfide nonahydrate (>98%), cobalt(II) bromide (99%), 2,6-diacetylpyridine (99%), bis(pinacolato)diboron (99%), 4,4′-di-*tert*-butyl bipyridine (dtbpy, 85%), tetrakis(triphenylphosphine)palladium (99%), and bis(1,5-cyclooctadiene)diiridium(I)-dimethoxide ($[Ir(COD)(OMe)]_2$, 96%) were purchased from Aladdin®. The intermediate, di-*tert*-butyl 4-chloropyridine-2,6-dicarboxylate, was synthesized according to the previously reported method.[S1] The reference catalyst, cobalt(III) tetraazamacrocyclic complex (**C2**), and $CuInS_2$/ZnS core-shell quantum dots (QDs) were synthesized according to published procedures.[S2,S3] Other commercially available reagents were used as received. Organic solvents of analytical reagent grade were used without further purification. All synthetic manipulations were carried out under N_2 with standard Schlenk techniques. Highly pure water (18.2 $M\Omega \cdot cm^{-1}$) supplied by a Milli-Q system (Millipore, Direct-Q 3 UV) was used in all related experiments.

Characterization methods

UV-vis absorption measurements were carried out on an Agilent 8453 spectrophotometer. Photoluminescence spectra were recorded using an FluoroMax-4P fluorimeter (Horiba Jobin Yvon Inc.). Transmission electron microscope (TEM) images were recorded on an FEI Tecnai G2 F20 S−TWIN instrument. X-ray photoelectron spectra (XPS) were obtained on an ESCALAB 250Xi (Thermo Scientific™). Raman spectra were measured with a DXR Microscope (Thermo Fisher™). Inductively coupled plasma-optical emission spectrometry (ICP-OES) analyses were measured on an Optima 2000 DV (PerkinElmer™). X-ray diffraction (XRD) was measured with a SmartLab (Rigaku™). ^{1}H-Nuclear magnetic resonance (NMR) spectra were obtained on a Bruker DRX-500 instrument at 298 K. Mass

spectra (MS) were obtained on a MALDI micro MX instrument (Waters™).

Synthesis of catalyst C1

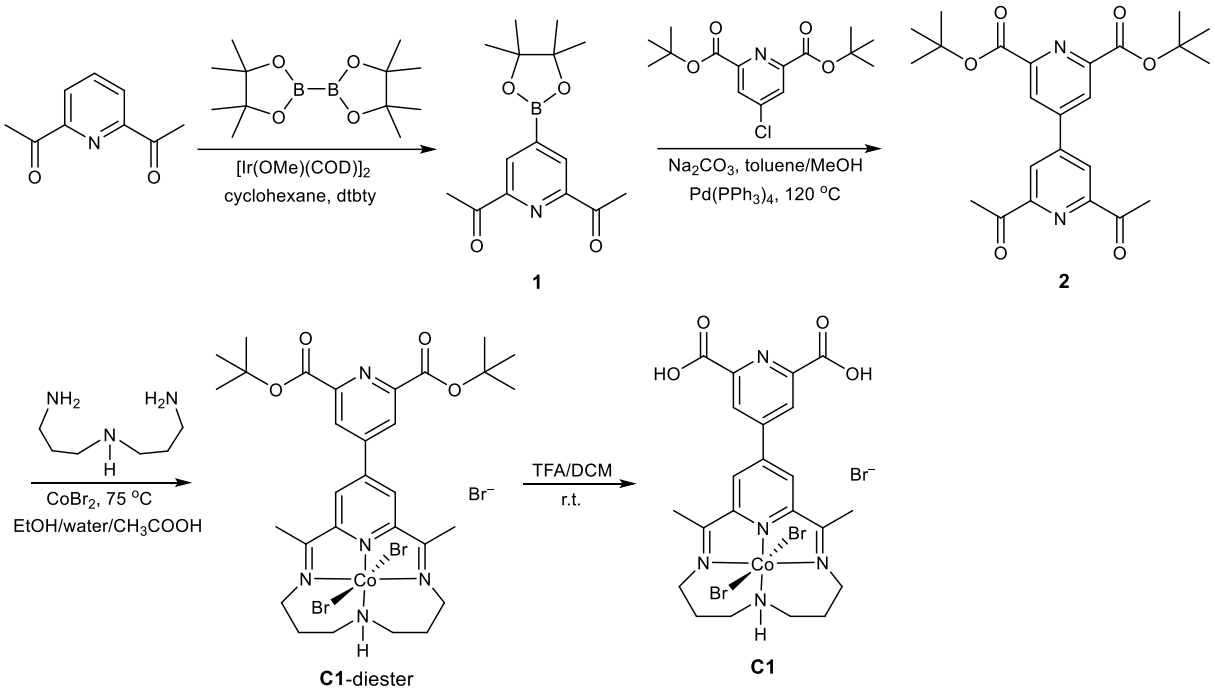

Scheme S1 Synthetic route for **C1**.

Synthesis of 1. 4-Pinacolboryl-2,6-diacetylpyridine (**1**) was synthesized according the reported protocol, namely an iridium-catalyzed C−H borylation reaction.[S4,S5] Compound dtbty (24 mg, 0.089 mmol) and $[Ir(OMe)(COD)]_2$ (30 mg, 0.045 mmol) were added to the cyclohexane (40 mL) in a 3-neck flask, and then bis(pinacolato)diboron (390 mg, 1.54 mmol) was added to the solution. After stirring for 15 min, diacetylpyridine (500 mg, 3.06 mmol) was added to the resulting mixture. Then the reaction was stirred and refluxed for 3 h under N_2. After removal of solvent, the crude product was purified by recrystallization in methanol (10 mL) at −10 °C. The crystalline solid was collected on a frit filter and washed with cold cyclohexane, yielding 813 mg (92%) of the desired product. ^{1}H NMR (500 MHz, $CDCl_3$): δ 8.55 (s, 2H), 2.79 (s, 6H), 1.36 (s, 12H) (Fig. S1).

Synthesis of 2. Di-*tert*-butyl 4-chloropyridine-2,6-dicarboxylate (626 mg, 2 mmol), **1**

(578 mg, 2 mmol), tetrakis(triphenylphosphine)palladium (115 mg, 0.1 mmol), and Na_2CO_3 (210 mg, 2 mmol) were added to the solution of toluene/MeOH (10:1, 10 mL).[S6,S7] The mixture was stirred for 12 h at 120 °C under Ar. After removal of the solvent, the residue was purified by chromatography using a silica-gel column with ethyl acetate and petroleum (1:10) as eluent. The intermediate **2** was isolated as white crystals in a yield of 72% (634 mg). ^{1}H NMR (500 MHz, $CDCl_3$): δ 8.54 (s, 2H), 8.48 (s, 2H), 2.86 (s, 6H), 1.68 (s, 18H) (Fig. S2).

Synthesis of C1-diester. Compound **2** (440 mg, 1.0 mmol) and $CoBr_2$ (249 mg, 1.0 mmol) were dissolved in the mixed solution of ethanol (6.3 mL) and water (4.2 mL), which was kept at 40 °C under Ar. The mixture was stirred at 55 °C to dissolve the cobalt salt, and a purple solution was obtained. Then 3,3′-diaminodipropylamine (0.59 mL, 4.2 mmol) and glacial acetic acid (0.1 mL) were added to the solution at 75 °C. The mixture became cloudy, and meanwhile, the color of the mixture turned to dark brown. After the mixture was stirred for 5 h at 75 °C, the concentrated HBr aqueous solution (1 mL) was added to the mixture with air blowing. The solution turned green and it was aerated for about 6 h. The complex **C1**-diester was precipitated as green microcrystals, which were filtered and washed with cold ethanol. The product was isolated in a yield of 39% (692 mg). ^{1}H NMR (500 MHz, CD_3OD): δ 8.97 (s, 2H), 8.76 (s, 2H), 6.51 (s, 1H), 4.24 (d, J = 17.6 Hz, 2H), 3.70 (t, J = 13.2 Hz, 2H), 3.54–3.48 (m, 2H), 3.16 (m, 2H), 3.02 (s, 6H), 2.32 (broad, 4H), 1.69 (s, 18H) (Fig. S3).

Synthesis of C1. The green crystals of **C1**-diester (834 mg, 1.0 mmol) were dissolved in a mixed solvent of trifluoroacetic acid/CH_2Cl_2 (*V*/*V*, 1:2; 6 mL), and the mixture was stirred for 12 h at room temperature. The desired product was collected as green precipitate, which was washed with cold ethanol and dried in vacuum. Complex **C1** was obtained in a yield of 85% (610 mg). MS (ESI) calcd for $[M–Br]^+$ ($C_{22}H_{25}Br_2CoN_5O_4$): m/z = 641.96, found: 642.01. ^{1}H NMR (500 MHz, DMSO-d_6): δ 13.83 (br s, 2H), 9.21 (s, 2H), 9.02 (s, 2H), 6.74 (t, J = 9.5 Hz, 1H), 4.24 (d, J = 10.8 Hz, 2H), 3.62–3.55 (m, 4H), 3.25 (t, J = 9.5 Hz, 2H), 3.08 (s, 6H), 2.29 (d, J = 12.8 Hz, 2H), 2.11 (m, 2H) (Fig. S4). ^{13}C NMR (125.8 MHz, CD_3OD): δ 180.20,

166.98, 159.68, 151.27, 150.75, 148.26, 127.61, 127.23, 52.93, 51.94, 27.56, 17.99 (Fig. S5).

Crystallographic structure determination of C1-diester

The single-crystal X-ray diffraction data were collected on a Bruker Smart Apex II CCD diffractometer with a graphite-monochromated Mo-K_α radiation (λ = 0.071073 Å) at 293 K using the ω-2θ scan mode. Data processing was accomplished with the SAINT processing program.[S8] Intensity data were corrected for absorption by the SADABS program.[S9] All structures were solved by direct methods and refined on F^2 against full-matrix least-squares methods by using the SHELXTL 97 program package.[S10] Non-hydrogen atoms were refined anisotropically. Hydrogen atoms were located by geometrical calculation. The single crystal X-ray structure of **C1**-diester is shown in Fig. 2. The crystallographic data and processing parameters are given in Table S1, and the selected bond lengths and angles are summarized in Tables S2 and S3. CCDC 1899565 contains the supplementary crystallographic data for **C1**-diester. The data can be obtained free of charge from the Cambridge Crystallographic Data Centre.

Electrochemistry

Electrochemical measurements were recorded in a three-electrode cell under argon using a CHI650E electrochemical workstation. A glassy carbon electrode was used as the working electrode, a Ag/AgCl as the reference electrode, and a Pt wire as the counter electrode. A 0.5 M NaHA/H_2A aqueous solution at pH 4.5 and a 0.1 M Na_2SO_4 solution were used as electrolytes with a scan rate of 100 mV s^{-1}. All the experimentally measured potentials were converted to the ones versus normal hydrogen electrode (NHE) by the equation: E_{NHE} = +0.197 V vs Ag/AgCl.

Electrochemical reduction of C1 and C2 (from Co^{3+} to Co^{2+} state)

Catalysts in the Co^{2+} state, **C1**(Co^{2+}) and **C2**(Co^{2+}), were generated by electrochemical reduction. A degassed solution containing catalyst either **C1**(Co^{3+}) or **C2**(Co^{3+}) (1.0 mM) and Na_2SO_4 (0.1 M) was added to one chamber of an H-cell, which had two chambers separated by a frit. A glassy carbon (10 mm × 10 mm) was used as the working electrode, and a Ag/AgCl as the reference electrode, which were put into a chamber containing the cobalt catalyst. A Pt mesh was used as the counter electrode and placed in the other chamber which did not contain catalyst. A potential of −0.2 V vs NHE was applied on the working electrode. After 15 min of electrolysis with stirring, the color of the reaction mixture changed from light yellow to green, indicative of formation of **C1**(Co^{2+}) or **C2**(Co^{2+}).

Collecting precipitates from the C1/CISZ QDs and C2/CISZ QDs colloids

The solution of the cobalt catalyst **C1** or **C2** (2 mL, 0.4 mM) was added to the CISZ QDs colloid (2 mL, 0.8 mM). After the mixture was stirred at room temperature for 2 h, isopropanol (10 mL) was added to the resulting solution. Particles were precipitated, which were collected by high speed centrifugation (8000 rpm), washed with diethyl ether, and dried at 60 °C for 8 h. The loading amount of **C1** on the QDs for **C1**@CISZ was analyzed by ICP technique, the proportion of **C1** to CISZ QDs was (8.3±0.4)% (mol/mol). For the particles collected from the **C2**/CISZ colloid, only trace amount of Co was detected by XPS analysis (Fig. S7c).

Photocatalysis

The photocatalytic reactions were carried out with either in situ generated or isolated **C1**@CISZ, or the mixture of **C2** and CISZ QDs as photocatalysts in 0.5 M NaHA/H_2A buffer solutions (pH 4.5) at 25 ºC under illumination of a Xe lamp (150 W, fitted with λ > 400 nm cutoff filter). The gas phase of the reaction system was analyzed by a gas chromatography

(TECHCOMP GC7890T, with a thermal conductivity detector, a 5 Å molecular sieve column with argon as the carrying gas). The amount of hydrogen generated was determined by the external standard method and the hydrogen dissolved in the solution was neglected.

Calculation of TON

TON (turnover number) was calculated by the following equation:

$$\mathrm{TON_{cat}} = \frac{n_{\mathrm{H_2}}}{n_{\mathrm{cat}}} = \frac{V_{\mathrm{H_2}} / V_{\mathrm{m,H_2,25\,^oC}}}{n_{\mathrm{cat}}}$$

Where the V_{H_2} is the volume of generated hydrogen (mL, determined by fitting the area of H_2 in GC to an external standard), the $V_{m,H_2,25°C}$ is the molar volume of gas at 25 °C (22.4 mL $mmol^{-1}$).

Measurements and calculations of quantum yields

A typical example of the photocatalytic reactions for evaluation of apparent and internal quantum yields (AQY and IQY) is given below. The photocatalytic HER was carried out in a schlenk bottle (25 mL), and the aqueous solution (5 mL) containing CISZ QDs (4.2×10^{-4} M), **C1** (4.0×10^{-5} M), and NaHA/H_2A (0.5 M) at pH 4.5 was deoxygenated by bubbling with Ar for 45 min before photolysis. The mixture was stirred under illumination (area = 1 cm^2, path-length = 1 cm) with a monochromatic LED light source (λ = 420 nm), and the accurate illumination power was measured by using a digital photodiode power meter (THORLABS, model PM100-D). The number of absorbed photons was calculated from the illumination power and the absorbance of CISZ QDs in the reaction solution, and the amount of hydrogen evolved from the solution was determined by GC analysis. The intensity of the illumination power was 57(±1) mW cm^{-2}, and the absorbance of CISZ QDs in the reaction solution under illumination (λ = 420 nm) was 0.366(±0.003). Based on the results obtained from three independent experiments, AQY and IQY were calculated as the reported method:[S11]

Molar amount of H_2 evolved during 3600 s of photolysis: 1.1×10^{-5} mol

H_2 generation rate: $k = n_{H_2} / t = 3.05 \times 10^{-9}$ mol s^{-1}

Percentage of absorbed photons: $T_a = 1 - 10^{-abs} = 1 - 10^{-0.366} = 0.57$

Amount of incident photons per second: $q_p = P\lambda / ch = [(0.057\ J\ s^{-1}) \times (420 \times 10^{-9}\ m)] / [(3.0 \times 10^{8}\ m\ s^{-1}) \times (6.626 \times 10^{-34}\ J\ s^{-1})] = 1.20 \times 10^{17}\ s^{-1} = 2.0 \times 10^{-7}$ mol s^{-1}

$\Phi_{H_2}(AQY) = 2k / q_p = 2 \times (3.05 \times 10^{-9}\ mol\ s^{-1}) / (2.0 \times 10^{-7}\ mol\ s^{-1}) = 3.05\%$

$\Phi_{H_2}(IQY) = \Phi_{H_2}(AQY) / T_a = 3.05 / 0.57 = 5.35\%$

The calculated AOYs and IQYs for different hybrid systems are summarized in Table S4.

Time-resolved photoluminescence (PL) measurements

Time-resolved PL spectra were measured using an ultrafast fluorescence lifetime spectrometer with ~200 ps temporal resolution (TemPro-01). The aqueous solutions of CISZ QDs were diluted to ensure that their optical densities were lower than 0.1 at emission wavelengths, and the diluted solutions were sealed in custom-made airtight cuvettes (optical path 1 cm) for measurements. Samples were excited at 400 nm with 1.2 ns pulse width and 1 MHz repetition rate. Neutral density filters were used to vary the power of the excitation pulse. PL decay curves were obtained by time-correlated single-photon counting mode. Lifetimes were obtained from a multi-exponential fit of the decay curve. All measurements were conducted under nitrogen protection to avoid the effect of oxygen.

TA experiment set-ups

The femtosecond pump-probe TA measurements were performed using a regenerative amplified Ti:sapphire laser system (Coherent; 800 nm, 70 fs, 6 mJ/pulse, and 1 kHz repetition rate) as the laser source and a femto-TA100 spectrometer (Time-Tech Spectra). Briefly, the

800 nm output pulse from the regenerative amplifier was split in two parts with a 50% beam splitter. The transmitted part was used to pump a TOPAS Optical Parametric Amplifier (OPA), which generated a wavelength-tunable laser pulse from 250 nm to 2.5 μm as pump beam. The reflected 800 nm beam was split again into two parts. One part with less than 10% was attenuated with a neutral density filter and focused into a 2 mm thick sapphire window to generate a white light continuum (WLC) used for probe beam. The probe beam was focused with an Al parabolic reflector onto the sample. The probe beam having passed through the sample was collimated and then focused into a fiber-coupled spectrometer with CMOS sensors, and detected at a frequency of 1 KHz. The intensity of the pump pulse used in the experiments was controlled by a variable neutral-density filter wheel. The delay between the pump and probe pulses was controlled by a motorized delay stage. The pump pulses were chopped by a synchronized chopper at 500 Hz, and the absorbance change was calculated with two adjacent probe pulses (pump-blocked and pump-unblocked). The samples were placed in 1 mm airtight cuvettes and measured under ambient conditions.

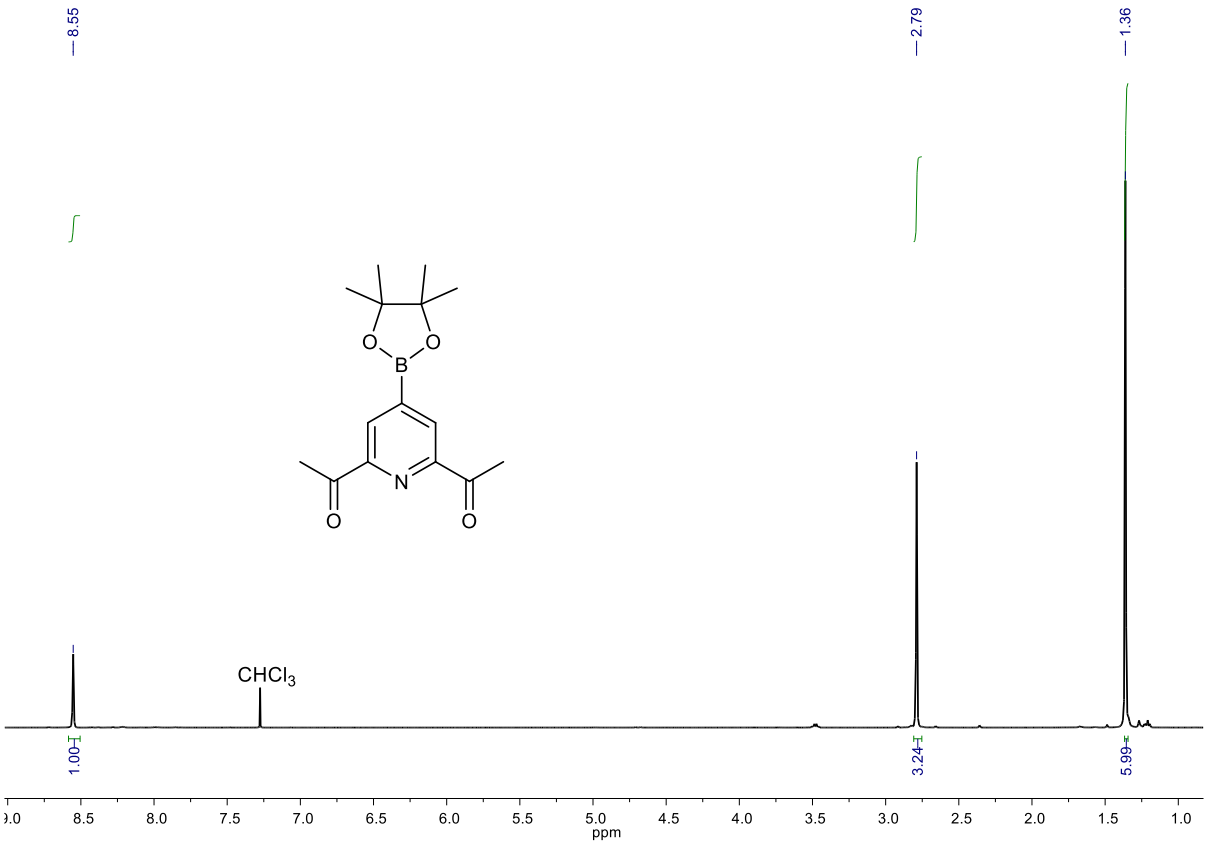

Fig. S1 ^{1}H NMR spectrum of **1** in $CDCl_3$.

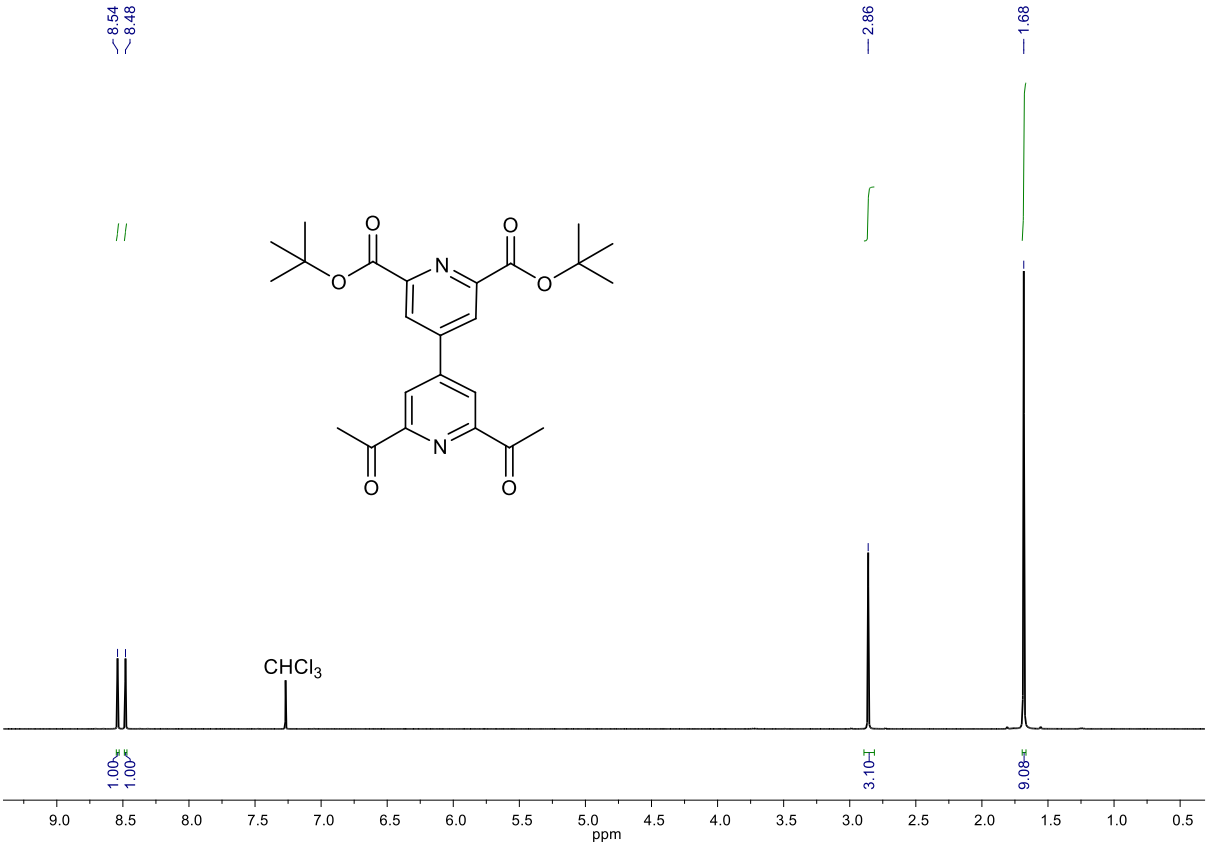

Fig. S2 ^{1}H NMR spectrum of **2** in $CDCl_3$.

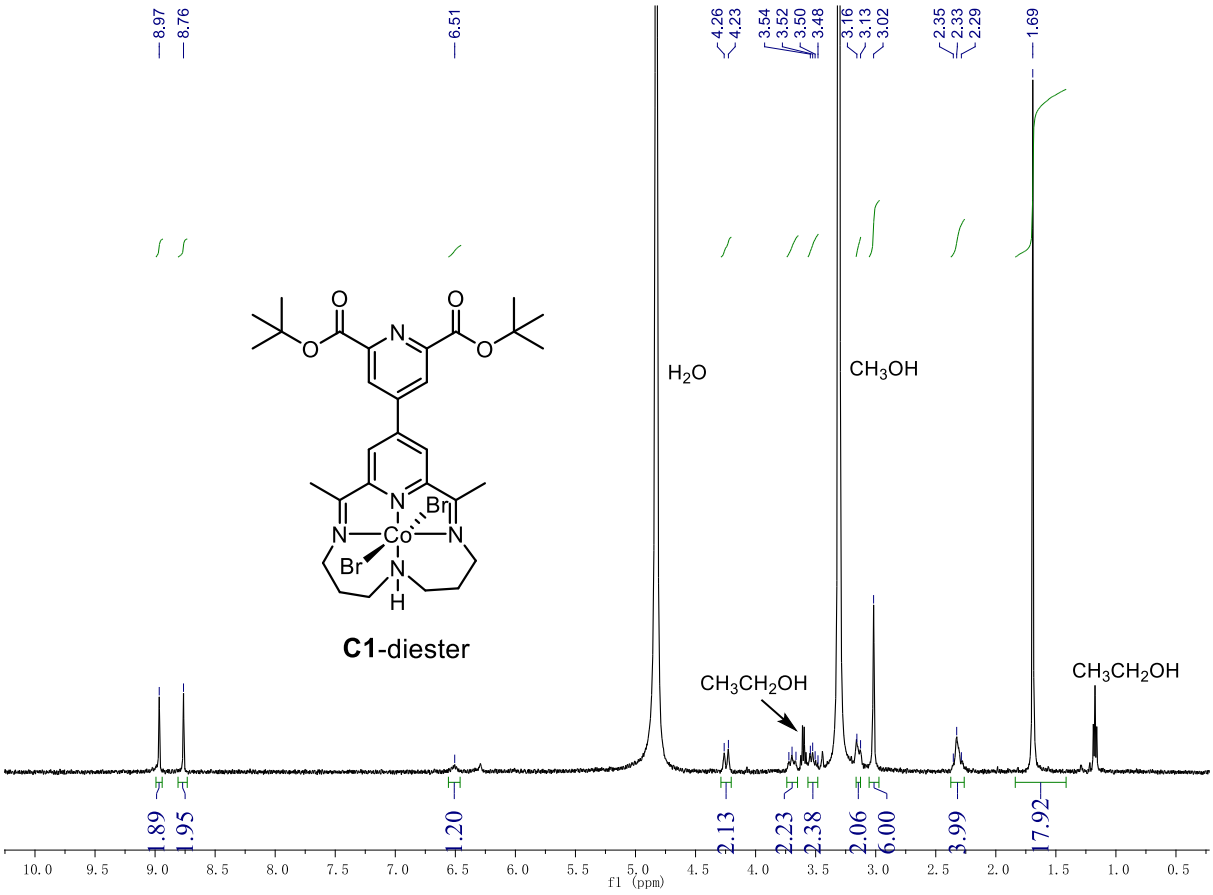

Fig. S3 ^{1}H NMR spectrum of **C1**-diester in CD_3OD/D_2O.

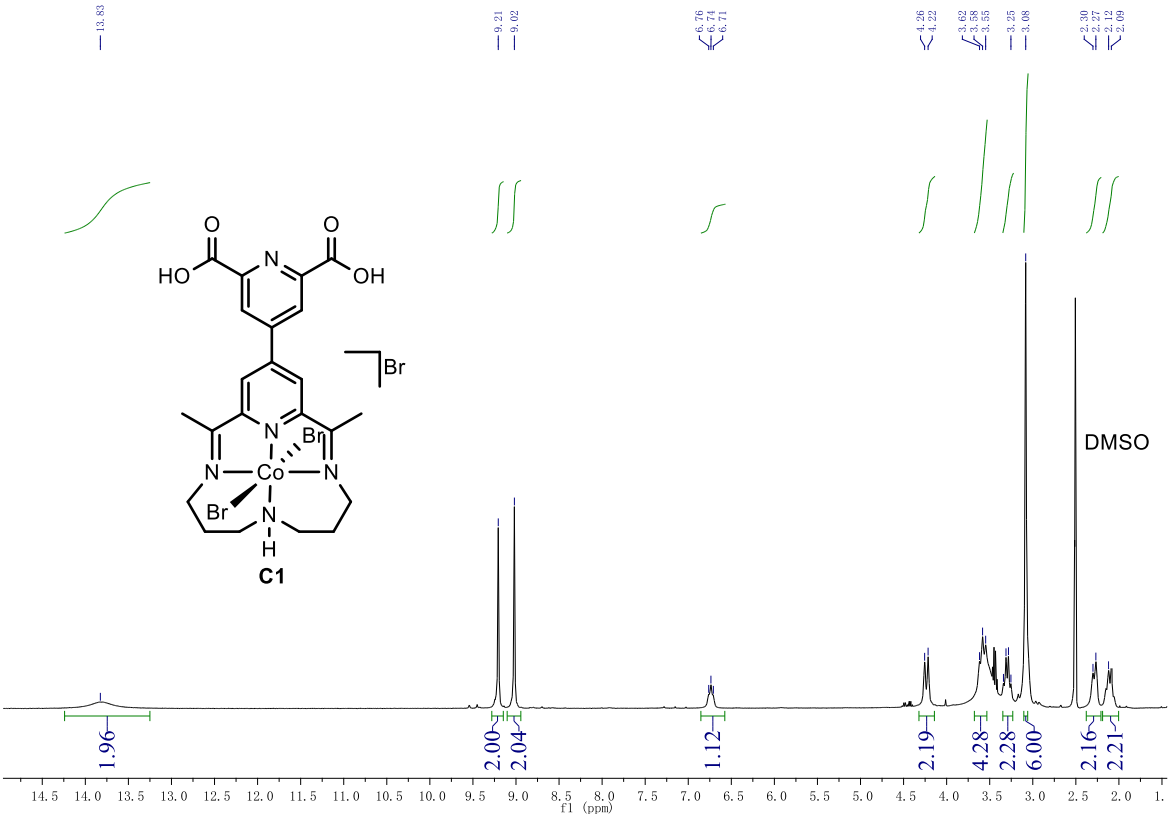

Fig. S4 ^{1}H NMR spectrum of **C1** in DMSO-d_6.

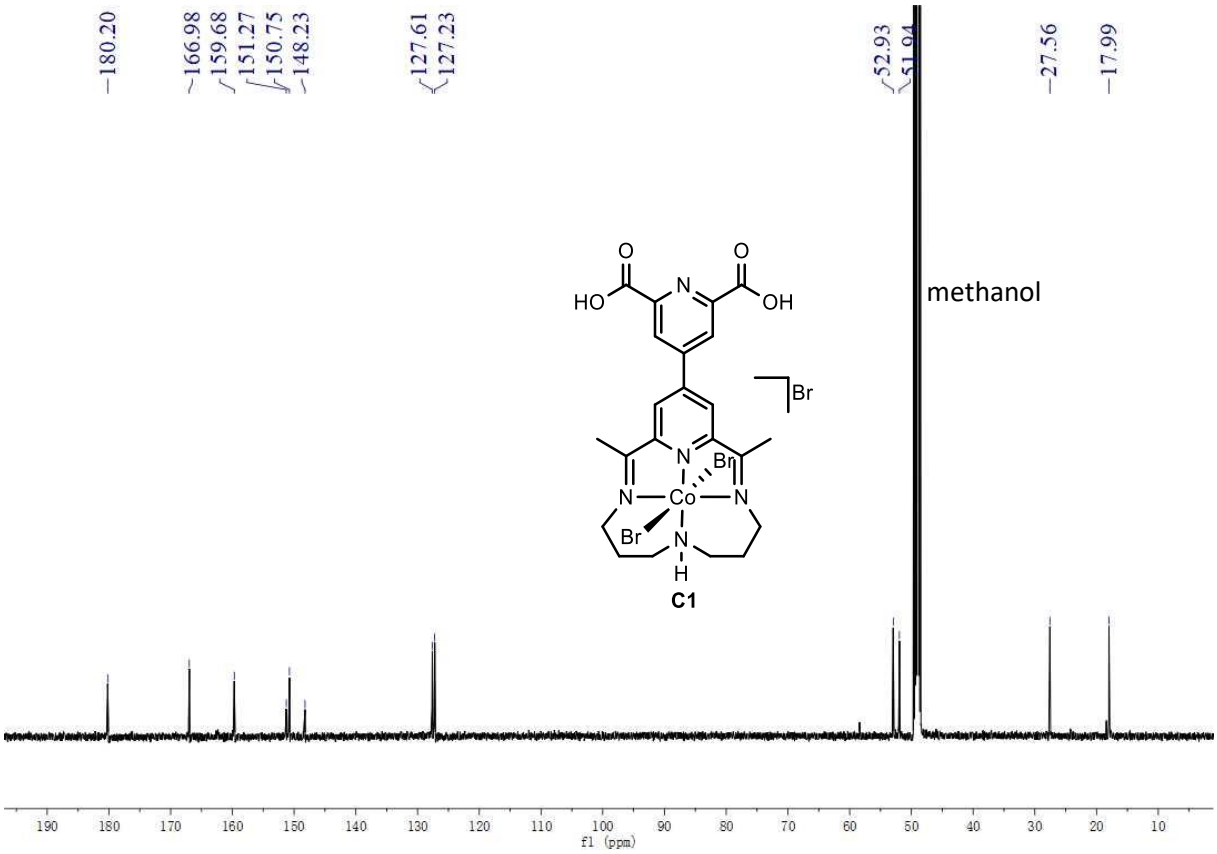

Fig. S5 ^{13}C NMR spectrum of **C1** in CD_3OD.

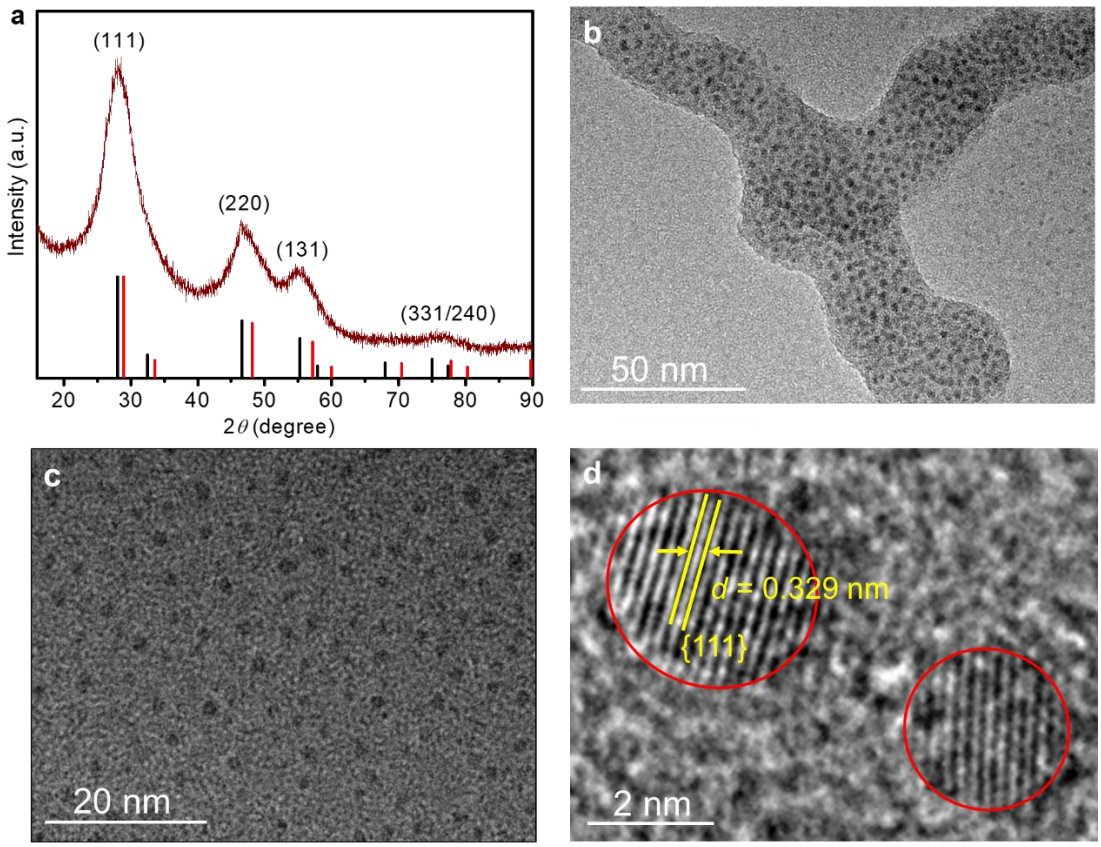

Fig. S6 (a) PXRD pattern of the as-prepared CISZ QDs compared with the data of $CuInS_2$ from JCPDS Card No. 47-1372 (black bars) and ZnS from JCPDS Card No. 80-0020 (red bars). (b),(c),(d) HRTEM images of as-prepared CISZ QDs in different scale bars.

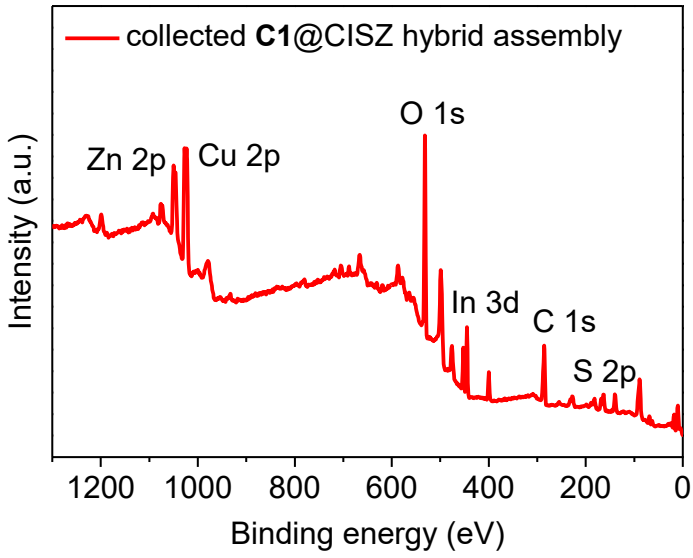

Fig. S7 XPS of the collected **C1**@CISZ QDs.

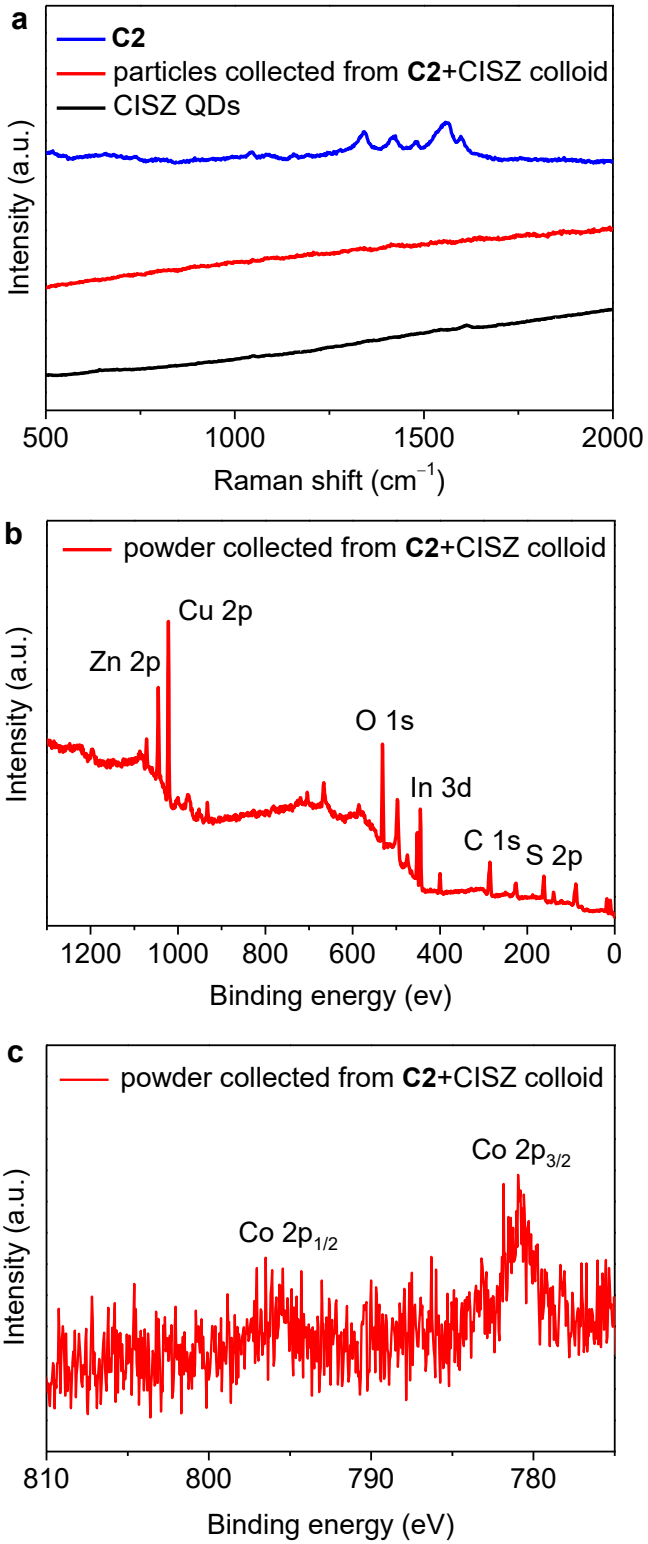

Fig. S8 (a) Raman spectra of **C2**, CISZ QDs, and the fine powder collected from the colloid of **C2** and CISZ QDs. (b) XPS of the powder collected from the colloid of **C2** and CISZ QDs. (c) High-resolution XPS of the Co 2p region.

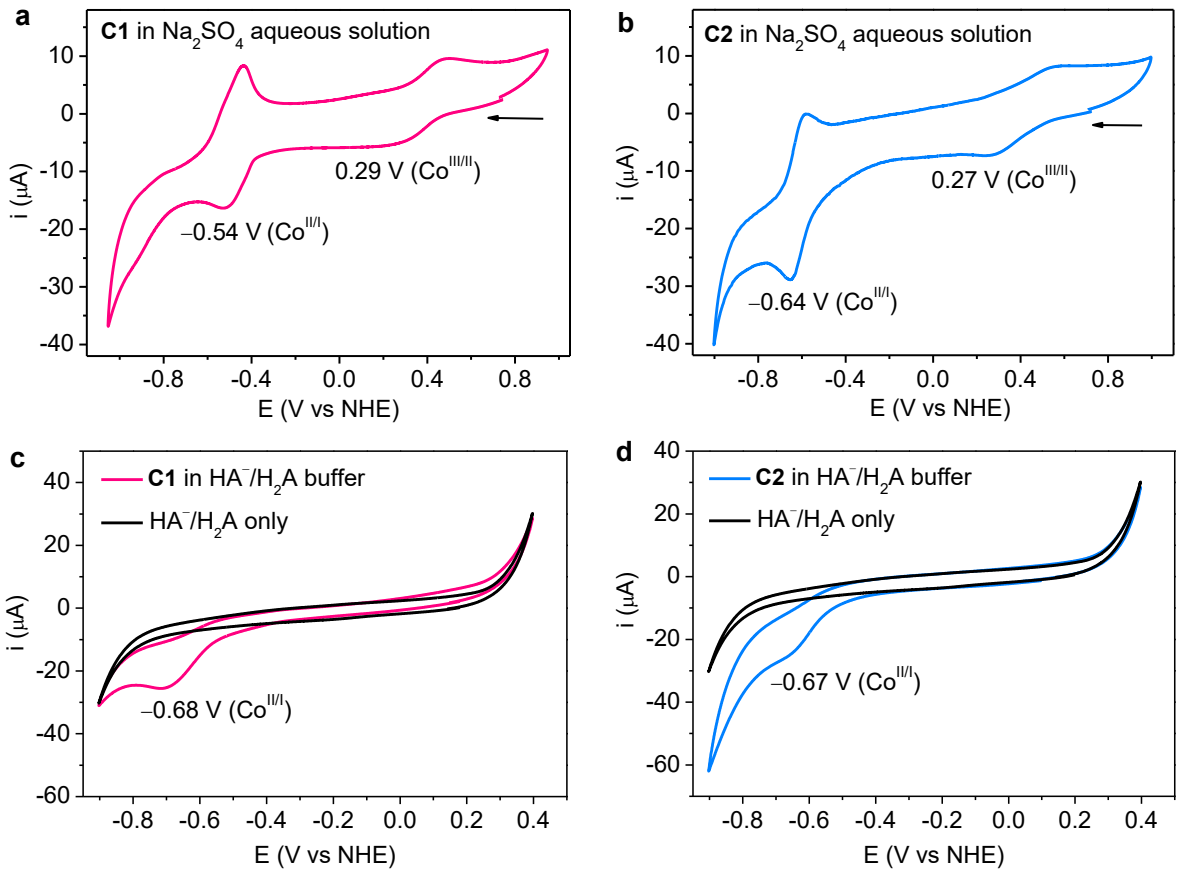

Fig. S9 Cyclic voltammograms of (a) **C1** and (b) **C2** (both in 1.0 mM) measured in 0.1 M Na_2SO_4 aqueous solutions in a scan rate of 100 mV s^{-1} with a glassy carbon as working electrode, a Ag/AgCl as reference electrode, and a Pt wire as counter electrode. Cyclic voltammograms of (c) **C1** and (d) **C2** measured in 0.5 M NaHA/H_2A buffer at pH 4.5.

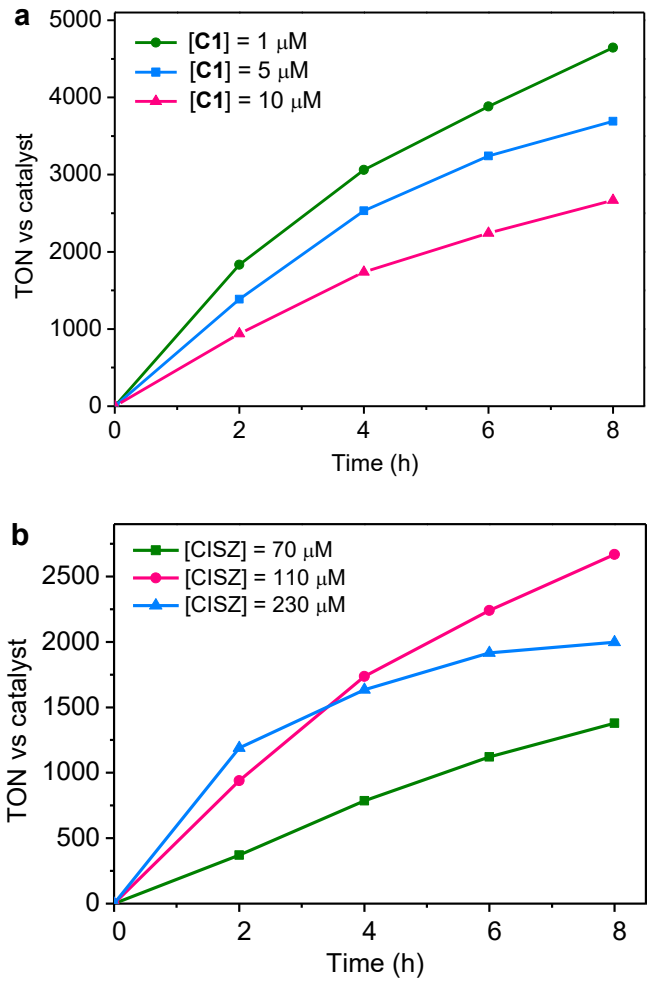

Fig. S10 Photocatalytic H_2 evolution (a) from **C1**@CISZ formed in situ with [CISZ] = 110 μM and [**C1**] = 1, 5 and 10 μM, and (b) from **C1**@CISZ formed in situ with [**C1**] = 10 μM and [CISZ] = 70, 110 and 230 μM in deaerated aqueous solutions containing 0.5 M H_2A/HA^- at pH 4.5.

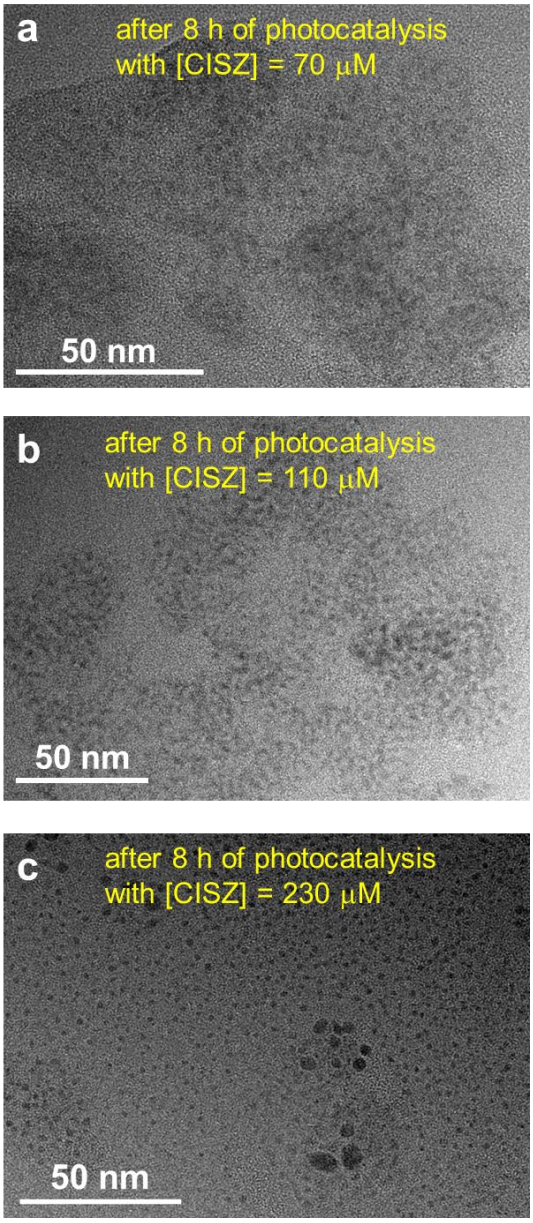

Fig. S11 TEM images of the CISZ QDs after 8 h of photocatalysis with [CISZ] = 70 μM (a), 110 μM (b), 230 μM (c) and [**C1**] = 10 μM in 0.5 M H_2A/HA^- aqueous solutions at pH 4.5.

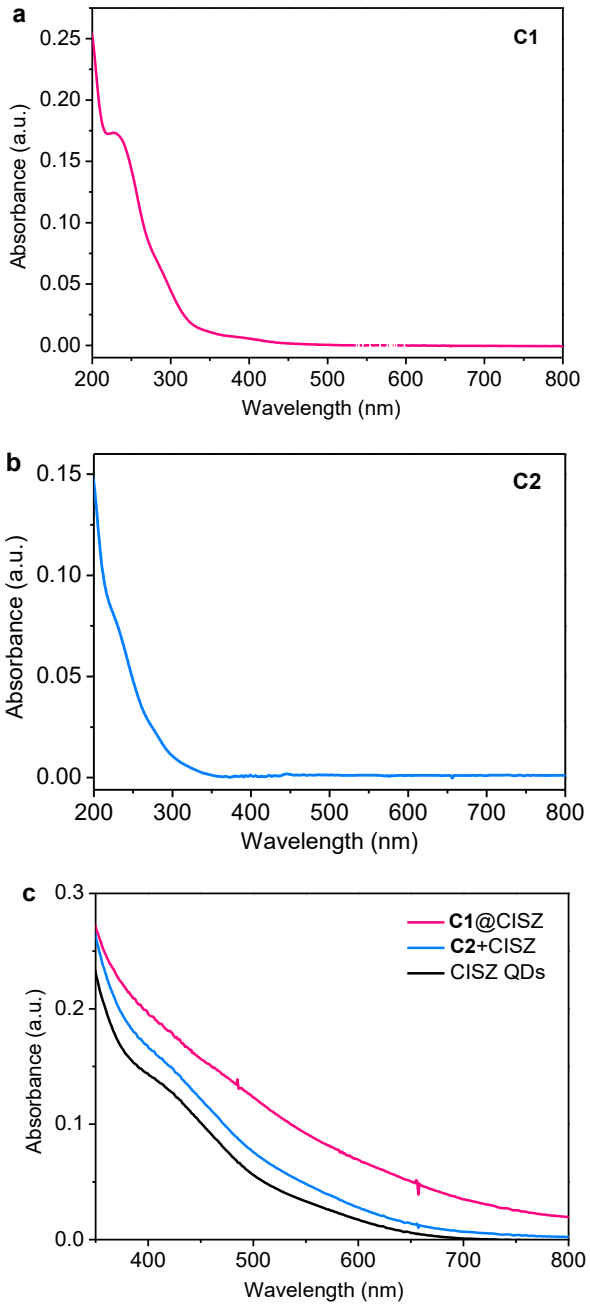

Fig. S12 UV-vis spectra of (a) **C1**, (b) **C2**, and (c) CISZ QDs, **C2**+CISZ, and **C1**@CISZ in AcOH/AcONa aqueous solutions at pH 4.5 with CISZ QDs (110 μM), **C1** and **C2** (both in 10 μM).

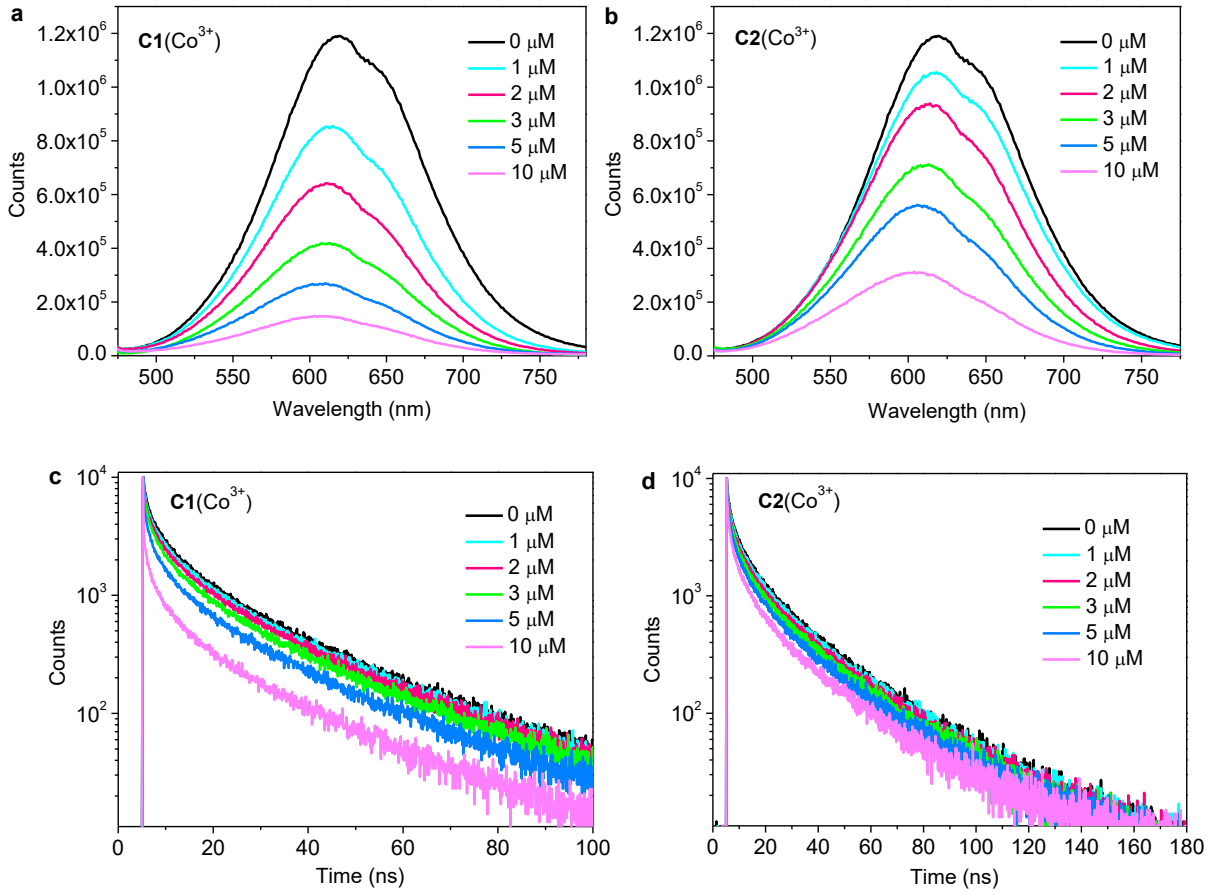

Fig. S13 Emission spectra of CISZ QDs (110 μM) with different concentrations of (a) **C1**(Co^{3+}) and (b) **C2**(Co^{3+}). Photoluminescence decay curves of CISZ QDs by adding different portions of (c) **C1**(Co^{3+}) and (d) **C2**(Co^{3+}). The samples were excited at λ_{ex} = 400 nm and monitored at λ_{em} = 600 nm.

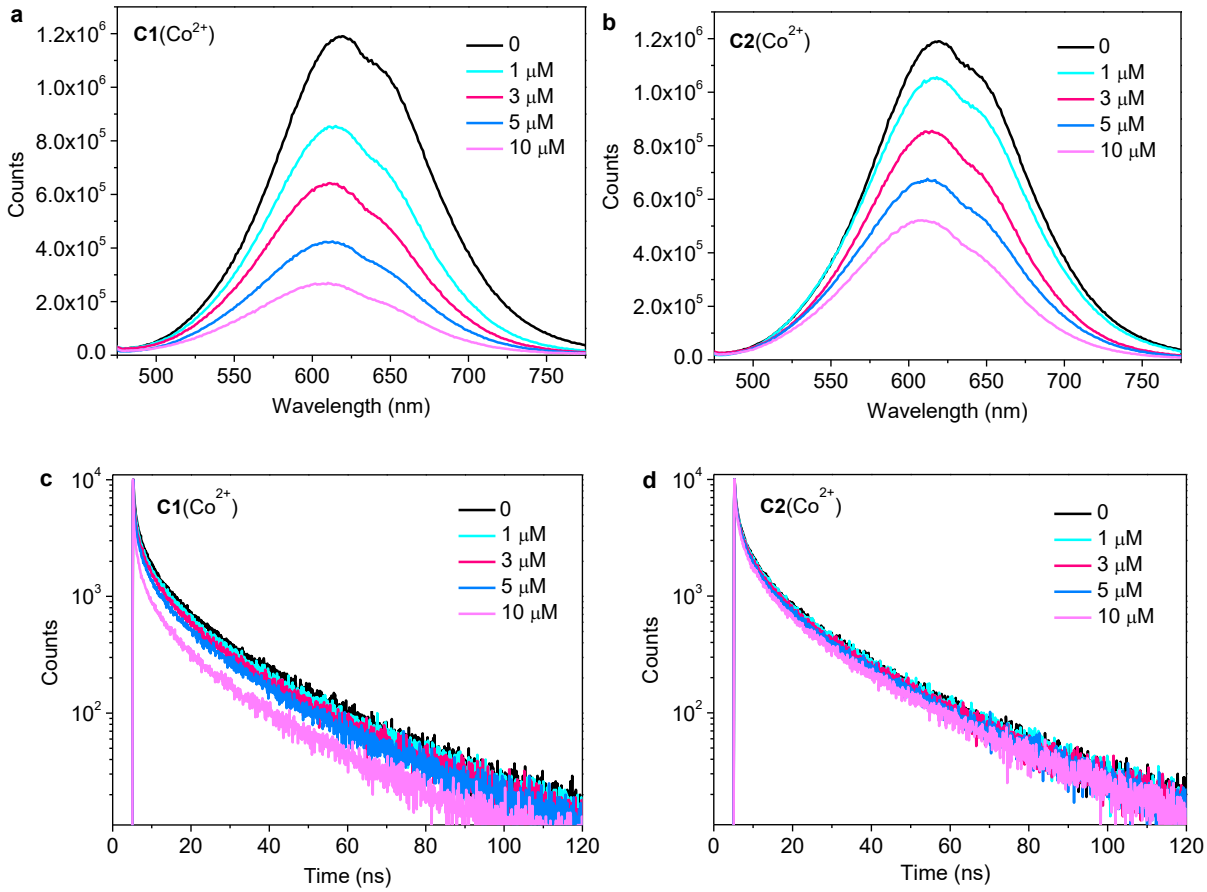

Fig. S14 Emission spectra of CISZ QDs (110 μM) with different concentrations of (a) **C1**(Co^{2+}) and (b) **C2**(Co^{2+}). Photoluminescence decay curves of CISZ QDs by adding different portions of (c) **C1**(Co^{2+}) and (d) **C2**(Co^{2+}). Before measurements, the catalysts were electrochemically reduced at −0.2 V for 15 min to obtain the Co^{2+} state of the catalysts. The samples were excited at λ_{ex} = 400 nm and monitored at λ_{em} = 600 nm.

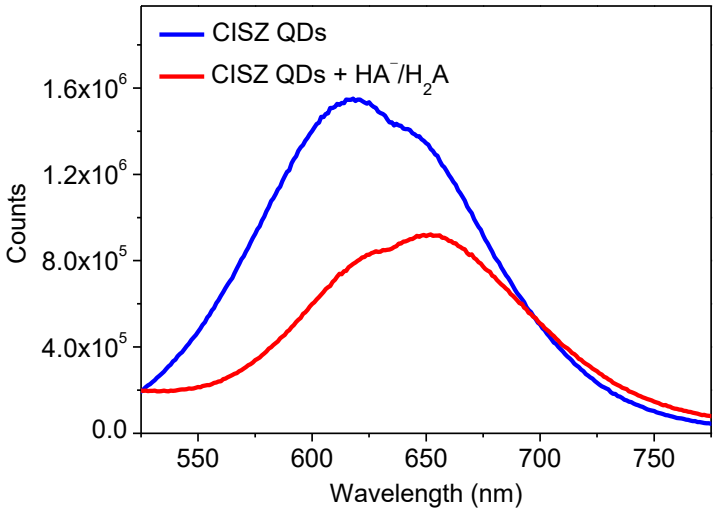

Fig. S15 PL spectra of CISZ QDs (110 μM) and QDs with the sacrificial electron donor (0.5 M HA^-/H_2A, excitation at 450 nm).

Table S1 Crystallographic data and processing parameters for **C1**-diester

Compound	**3**
Formula	$C_{30}H_{41}Br_3CoN_5O_4$
Formula weight	833.30
T / K	293(2)
Crystal system	Monoclinic
Space group	$P2_1/c$
a / Å	17.539(5)
b / Å	9.482(5)
c / Å	21.920(5)
α / deg	90.000(5)
β / deg	99.692(5)
γ / deg	90.000(5)
V / Å^3	3593(2)
Z	4
D_{calcd} / g cm^{-3}	1.541
μ / mm^{-1}	3.853
Crystal size / mm	0.24 × 0.18 × 0.14
2θ range for data collection / deg	3.76 to 55.16
Reflections collected	38824
Independent reflections	8323 (R_{int} = 0.1214, R_{sigma} = 0.1228)
Data/restraints/parameters	8323/0/388
F(000)	1676
GOF on F^2	0.997
Final R (I > = 2σ(I))	R_1 = 0.0708, wR_2 = 0.1752
Final R (all data)	R_1 = 0.1969, wR_2 = 0.2311
Max. peak/hole / e Å^{-3}	1.44 / −1.09

$R_1 = \Sigma||F_o| - |F_c||/\Sigma|F_o|$, $wR_2 = [\Sigma(|F_o|^2 - |F_c|^2)^2/\Sigma(Fo_2)]^{1/2}$

Table S2 Bond lengths (Å) of **C1**-diester

Br1–Co1	2.3831(18)	C25–C7	1.503(10)
Br2–Co1	2.3808(18)	C24–C19	1.384(10)
Co1–N2	1.843(6)	N4–C13	1.482(9)
Co1–N4	1.982(6)	N4–C9	1.510(10)
Co1–N5	1.949(6)	N5–C12	1.470(9)
Co1–N3	1.940(6)	C23–C19	1.403(11)
C30–C29	1.468(11)	C23–C18	1.397(11)
C30–C13	1.511(11)	C23–C14	1.479(11)
N2–C26	1.319(9)	C21–C11	1.405(11)
N2–C24	1.353(9)	C21–C5	1.474(13)
O4–C27	1.478(10)	C20–C16	1.383(11)
O4–C15	1.274(11)	C20–C15	1.522(12)
C29–N3	1.477(10)	C17–C12	1.495(11)
C28–C26	1.478(10)	C17–C9	1.495(12)
C28–N5	1.272(9)	C16–C14	1.377(11)
C28–C8	1.506(11)	C15–O2	1.211(10)
C27–C22	1.566(13)	O1–C10	1.492(14)
C27–C6	1.532(13)	O1–C5	1.321(11)
C27–C2	1.488(13)	C14–C11	1.387(11)
N1–C21	1.334(10)	C10–C4	1.537(17)
N1–C20	1.348(10)	C10–C3	1.478(18)
C26–C18	1.392(10)	C10–C1	1.436(18)
C25–C24	1.474(11)	O3–C5	1.196(11)
C25–N3	1.287(10)		

Table S3 Bond angles (deg) of **C1**-diester

Br2–Co1–Br1	178.73(6)	O4–C27–C22	100.4(8)
N2–Co1–Br1	90.98(19)	O4–C27–C6	108.5(8)
N2–Co1–Br2	88.10(19)	O4–C27–C2	111.2(8)
N2–Co1–N4	176.8(3)	C6–C27–C22	108.9(9)
N2–Co1–N5	81.4(3)	C2–C27–C22	110.8(9)
N2–Co1–N3	81.6(3)	C2–C27–C6	115.9(10)
N4–Co1–Br1	92.18(19)	C21–N1–C20	117.7(7)
N4–Co1–Br2	88.74(19)	N2–C26–C28	111.1(7)
N5–Co1–Br1	87.67(19)	N2–C26–C18	120.1(7)
N5–Co1–Br2	93.06(19)	C18–C26–C28	128.8(7)
N5–Co1–N4	98.1(3)	C24–C25–C7	118.2(8)
N3–Co1–r1	89.02(19)	N3–C25–C24	114.9(7)
N3–Co1–Br2	89.98(19)	N3–C25–C7	126.9(8)
N3–Co1–N4	99.1(3)	N2–C24–C25	109.5(7)
N3–Co1–N5	162.6(3)	N2–C24–C19	119.9(7)
C29–C30–C13	116.8(8)	C19–C24–C25	130.6(8)
C26–N2–Co1	118.2(5)	C13–N4–Co1	114.6(5)
C26–N2–C24	122.8(7)	C13–N4–C9	109.9(6)
C24–N2–Co1	118.7(5)	C9–N4–Co1	116.5(5)
C15–O4–C27	119.0(8)	C28–N5–Co1	114.9(5)
N3–C29–C30	114.1(7)	C28–N5–C12	120.0(7)
C26–C28–C8	118.3(7)	C12–5–Co1	124.5(5)
N5–C28–C26	114.0(7)	C29–N3–Co1	124.6(5)
N5–C28–C8	127.4(7)	C25–N3–Co1	115.0(5)

Table S4 AQYs and IQYs for photocatalytic H_2 evolution from the as-prepared hybrid systems and bare CISZ QDs[a]

	Amount of H_2 over 1 h (μmol)	AQY (%)	IQY (%)
CISZ QDs	trace	–	–
Isolated **C1**@CISZ	12	3.33	5.84
C1@CISZ	11	3.05	5.35
C2+CISZ	6	1.65	2.89

[a] Light intensity = 57 mW cm^{-2}.

Table S5 Time constants (τ_i) and populations (A_i) for the exciton decay of QDs with catalysts **C1**(Co^{3+}) and **C2**(Co^{3+}) obtained from time-correlated single photon counting (TCSPC)

Sample	τ_{et} / ns	τ_1 / ns	τ_2 / ns	τ_3 / ns
CISZ QDs		7.35 (46.3%)	52.50 (35.7)	267.88 (18.0%)
C2(Co^{3+})+CISZ	1.19 (35.7%)	7.35 (35.3%)	52.50 (20.7%)	267.88 (8.2%)
C1(Co^{3+})@CISZ	0.61 (84.4%)	7.35 (8.6%)	52.50 (5.0%)	267.88 (2.0%)

Table S6 Time constants (τ_i) and populations (A_i) for the exciton decay of QDs with one-electron reduced catalysts **C1**(Co^{2+}) and **C2**(Co^{2+}) obtained from TCSPC

Sample	τ_{et} / ns	τ_1 / ns	τ_2 / ns	τ_3 / ns
CISZ QDs		7.03 (44.9%)	47.51 (35.3%)	250.56 (19.7%)
C2(Co^{2+})+CISZ	1.25 (39.0%)	7.03 (32.2%)	47.51 (21.0%)	250.56 (7.9%)
C1(Co^{2+})@CISZ	0.78 (74.9%)	7.03 (14.8%)	47.51 (7.7%)	250.56 (2.6%)

Table S7 Time constants (τ_i) and populations (A_i) for exciton decay of QDs with adding sacrificial electron donor (HA^-/H_2A) obtained from TCSPC

Sample	τ_{ht} / ns	τ_1 / ns	τ_2 / ns	τ_3 / ns
CISZ QDs		208.58 (21.8%)	39.58 (37.1%)	5.21 (41.1%)
QDs + HA^-/H_2A	6.47	208.58 (10.1%)	39.58 (36.0%)	5.21 (53.9%)

Table S8 Time constants (τ_i) and populations (A_i) for exciton decay of QDs with **C1** and **C2** obtained from femtosecond TA measured in 0.5 M HA^-/H_2A aqueous solutions

Sample	τ_1 / ps	τ_2 / ps	τ_3 / ps
CISZ QDs	6.9 (36.0%)	82.0 (22.3%)	> 8000 (41.7%)
C2+CISZ	7.6 (30.7%)	84.7 (40.7%)	2083 (33.2%)
C1@CISZ	5.8 (19.1%)	143.0 (57.6%)	1282 (23.3%)

References

S1 F. Li, K. Fan, B. Xu, E. Gabrielsson, Q. Daniel, L. Li and L. Sun, *J. Am. Chem. Soc.*, 2015, **137**, 9153–9159.

S2 K. M. Long and D. H. Busch, *J. Coord. Chem.*, 1974, **4**, 113–123.

S3 M. Sandroni, R. Gueret, K. D. Wegner, P. Reiss, J. Fortage, D. Aldakov and M. N. Collomb, *Energy Environ. Sci.*, 2018, **11**, 1752–1761.

S4 J. Takagi, K. Sato, J. F. Hartwig, T. Ishiyama and N. Miyaura, *Tetrahedron Lett.*, 2002, **43**, 5649–5651.

S5 M. A. Larsen and J. F. Hartwig, *J. Am. Chem. Soc.*, 2014, **136**, 4287–4299.

S6 B. Su, J. Zhao, Y. Cui, Y. Liang and W. Sun, *Synth. Commun*., 2005, **35**, 2317–2324.

S7 C. H. Lee, D. Villágran, T. R. Cook, J. C. Peters and D. G. Nocera, *ChemSusChem*, 2013, **6**, 1541–1544.

S8 G. M. Sheldrick, *SHELXTL97 Program for the Refinement of Crystal Structure*, University of Göttingen, Germany, 1997.

S9 *Software packages SMART and SAINT*, Siemens Energy & Automation Inc., Madison, Wisconsin, 1996.

S10 G. M. Sheldrick, *SADABS Absorption Correction Program*, University of Göttingen, Germany, 1996.

S11 S. Yu, X.-B. Fan, X. Wang, J. Li, Q. Zhang, A. Xia, S. Wei, L.-Z. Wu, Y. Zhou and G. R. Patzke, *Nat. Commun.*, 2018, **9**, 4009.